


Simultaneous fermion and exciton condensations from a model Hamiltonian

LeeAnn M. Sager¹ and David A. Mazziotti^{1*}

Department of Chemistry and The James Franck Institute, The University of Chicago, Chicago, Illinois 60637, USA

 (Received 26 October 2021; accepted 3 January 2022; published 26 January 2022)

Fermion-exciton condensation in which both fermion-pair (i.e., superconductivity) and exciton condensations occur simultaneously in a single coherent quantum state has recently been conjectured to exist. Here, we capture the fermion-exciton condensation through a model Hamiltonian that can recreate the physics of this new class of highly correlated condensation phenomena. We demonstrate that the Hamiltonian generates the large-eigenvalue signatures of fermion-pair and exciton condensations for a series of states with increasing particle numbers. The results confirm that the dual-condensate wave function arises from the entanglement of fermion-pair and exciton wave functions, which we previously predicted in the thermodynamic limit. This model Hamiltonian—generalizing well-known model Hamiltonians for either superconductivity or exciton condensation—can explore a wide variety of condensation behavior. It provides significant insights into the required forces for generating a fermion-exciton condensate, which will likely be invaluable for realizing such condensations in realistic materials with applications from superconductors to excitonic materials.

DOI: [10.1103/PhysRevB.105.035143](https://doi.org/10.1103/PhysRevB.105.035143)

I. INTRODUCTION

Model Hamiltonians are theoretical tools that are often useful in simulating the key physics associated with large-scale, highly correlated systems. They are capable of modeling an array of quantum phases and many-body phenomena such as phase transitions [1–5], superconductivity [6–10], quantum magnetism [11–14], exciton condensation [15–21], latticelike systems [22,23], etc. Additionally, model Hamiltonians which encompass nontrivial physics are often useful as benchmarks for theoretical tools such as many-body approximations [6,24–26].

Condensation phenomena—which are inherently highly correlated—have a long history of being computationally studied through the lens of model Hamiltonians as traditional band theory is inaccurate for such highly entangled materials [6,7,10,15,27–29]. Specifically, superconductors—materials in which fermion-fermion (Cooper/electron-electron) pairs aggregate into a single quantum state, resulting in the superfluidity of the fermion-fermion pairs—are often explored through use of the pairing-force (PF) Hamiltonian [6–9], which is additionally referred to as the standard reduced Bardeen-Cooper-Schrieffer (BCS) Hamiltonian [10,25,30]. This Hamiltonian is a simple representation of superconductivity as it describes a system with bound Cooper (or Cooper-like particle-particle) pairs interacting in an attractive manner with the high-correlation limit of this Hamiltonian resulting in well-known, number-projected BCS wave functions [7,31]. Similarly, exciton condensation—in which particle-hole (exciton) pairs condense into a single quantum state resulting in the superfluidity of the composite excitons [32]—can be

modeled according to the Lipkin-Meshkov-Glick (LMG) Hamiltonian, which is often simply referred to as the Lipkin model [15–21,29,33]. This Hamiltonian is a highly degenerate system in which partnered orbitals are inherently particle-hole paired and whose strongly correlated form results in ground states that demonstrate character of exciton condensation.

Here, we introduce a model Hamiltonian that is capable of capturing fermion-exciton condensation, a new class of highly correlated condensation phenomena in which both fermion-pair and exciton condensations coexist in a single quantum state (see Fig. 1). We demonstrate such coexistent condensate character by calculating the quantum signatures of fermion-pair [34,35] and exciton [36,37] condensations (see Sec. II and Appendix A) for systems of even particle numbers ranging from $N = 4$ to 10 particles in $r = 2N$ orbitals. These fermion-exciton condensates are shown to be described by wave functions which are entanglements of wave

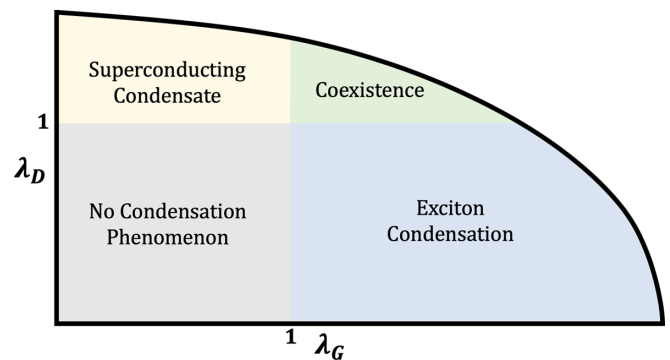


FIG. 1. A figure of the condensate phase diagram in the phase space of the signatures of particle-particle condensation, λ_D , and exciton condensation, λ_G , is shown. See Ref. [38] for the original figure.

*damazz@uchicago.edu

functions from BCS-like superconductivity and Lipkin-like exciton condensation—consistent with our prior predictions for the large- N thermodynamic limit [38] as well as those we observed experimentally on a quantum device [39].

Our determination of a model Hamiltonian that supports fermion-exciton condensation provides information regarding the nature of the forces necessary to generate such systems—an invaluable first step in the realization of real-world systems that support such dual condensation of excitons and fermion-fermion pairs, which may demonstrate some sort of hybrid of the properties of superconductors and exciton condensates and hence have applications in energy transport and electronics. The extent of these different phases and the transitions between these phases can also be studied. Moreover, our Hamiltonian provides an important reference in order to determine whether a given many-body approximation is capable of measuring dual condensate character.

II. THEORY

A. Fermion-pair condensation

Superconductivity results from the condensation of bosonic fermion-fermion pairs [10,40–42] into a single geminal—a two-fermion function directly analogous to the one-fermion orbital [34,35,43–46]—at temperatures below a certain critical temperature. This condensation of fermion-pairs results in the superfluidity (i.e., frictionless flow) of the constituent particle-particle pairs [10,42,47,48]; if the fermionic pairs are composed of electrons (i.e., Cooper pairs), then these superfluid electron-electron pairs demonstrate superconductivity.

As was first demonstrated by Yang [34] and Sasaki [35], a computational signature of such superconducting states is a large eigenvalue in the particle-particle reduced density matrix (2-RDM), whose elements are given by

$${}^2D_{k,l}^{i,j} = \langle \Psi | \hat{a}_i^\dagger \hat{a}_j^\dagger \hat{a}_l \hat{a}_k | \Psi \rangle, \quad (1)$$

where $|\Psi\rangle$ is an N -fermion wave function and where \hat{a}_i^\dagger and \hat{a}_i are fermionic creation and annihilation operators for orbital i , respectively. As eigenvalues of the 2-RDM can be interpreted as the occupations of the two-fermion geminals [49], when the largest eigenvalue of the 2-RDM—the signature of particle-particle condensation, represented by λ_D —exceeds the Pauli-like limit of one ($\lambda_D > 1$), multiple fermion-fermion pairs occupy a single geminal and hence superconducting character is observed. This signature is known to directly probe the presence and extent of nonclassical (off-diagonal) long-range order [44]. (See the Appendix for more details on how the signature of superconductivity, λ_D , is computed.)

The Pairing-Force (PF) model [6–9]—also called the standard reduced Bardeen-Cooper-Schrieffer (BCS) model [10,25,30]—is known to exhibit superconducting character in the strong correlation limit and hence achieve a large λ_D . The Hamiltonian for the PF model is given in second quantization by

$$\mathcal{H}_{PF} = \frac{1}{2} \sum_{\sigma=\uparrow,\downarrow} \sum_{p=1}^N \epsilon_p \hat{a}_{p,\sigma}^\dagger \hat{a}_{p,\sigma} - G \sum_{p=1}^N \sum_{q=1}^N \hat{a}_{p,\uparrow}^\dagger \hat{a}_{p,\downarrow}^\dagger \hat{a}_{q,\downarrow} \hat{a}_{q,\uparrow}, \quad (2)$$

where p is a quantum number that represents a pair of orbitals denoted as p, \uparrow and p, \downarrow with the same energy, where the energies (ϵ_p) are considered to be known, and where the parameter G is a constant that tunes the strength of the pairwise interactions. Note that in the limit of strong correlation ($G \gg \epsilon_p$), maximal superconducting character— $\lambda_D = \frac{N}{2}(1 - \frac{N-2}{r})$ [43,49]—is observed.

B. Exciton condensation

Directly analogous to superconductivity resulting from bosonic particle-particle pairs condensing into a single particle-particle function, exciton condensation results from the condensation of particle-hole pairs (i.e., excitons) into a single particle-hole function below a certain critical temperature, which results in the superfluidity of the excitons [32,50]. Exciton condensates, while difficult to realize experimentally, have been observed in systems composed of polaritons (excitons coupled to photons) [51–53] and in two-dimensional structures such as semiconductors [54], graphene bilayers [55–57], and van der Waals heterostructures [58–61].

The signature of exciton condensation—denoted as λ_G —is similarly analogous to that for fermion-pair condensation; the presence and extent of exciton condensate character can be measured from the largest eigenvalue of a modified particle-hole reduced density matrix given by [36,37,62]

$${}^2\tilde{G}_{k,l}^{i,j} = {}^2G_{k,l}^{i,j} - {}^1D_j {}^1D_k^l \\ = \langle \Psi | \hat{a}_i^\dagger \hat{a}_j \hat{a}_l^\dagger \hat{a}_k | \Psi \rangle - \langle \Psi | \hat{a}_i^\dagger \hat{a}_j | \Psi \rangle \langle \Psi | \hat{a}_l^\dagger \hat{a}_k | \Psi \rangle, \quad (3)$$

where 1D is the one-fermion reduced density matrix (1-RDM). Note that this modification removes the extraneous large eigenvalue from a ground-state-to-ground-state transition such that a signature above one ($\lambda_G > 1$) is indicative of exciton condensation. (See the Appendix for more details on how the signature of exciton condensation, λ_G is computed.) This computational signature has been utilized to study when exciton condensation is possible in quantum and molecular systems [29,37–39,63].

One model known to achieve a large λ_G value and hence exhibit exciton condensate character in the limit of a large correlation is the Lipkin quasispin model [15–21]. The N -fermion Lipkin quasispin model consists of two energy levels $\{-\frac{\epsilon}{2}, \frac{\epsilon}{2}\}$, each containing N energetically degenerate states. The second-quantized Hamiltonian can be expressed as [18]

$$\mathcal{H}_L = \frac{\epsilon}{2} \sum_{\sigma=\pm 1} \sigma \sum_{p=1}^N \hat{a}_{\sigma,p}^\dagger \hat{a}_{\sigma,p} \\ + \frac{\gamma}{2} \sum_{\sigma=\pm 1} \sum_{p,q=1}^N \hat{a}_{+\sigma,p}^\dagger \hat{a}_{-\sigma,p} \hat{a}_{-\sigma,q}^\dagger \hat{a}_{+\sigma,q} \\ + \frac{\lambda}{2} \sum_{\sigma=\pm 1} \sum_{p,q=1}^N \hat{a}_{+\sigma,p}^\dagger \hat{a}_{+\sigma,q}^\dagger \hat{a}_{-\sigma,q} \hat{a}_{-\sigma,p}, \quad (4)$$

where $\sigma = \pm 1$ and $p = 1, 2, \dots, N$ are quantum numbers that completely characterize the system in which p describes the site number labeling the N states in a given level and σ represents the upper (+1) or lower (−1) energy levels, respectively. Note that in this model, the λ term allows for double

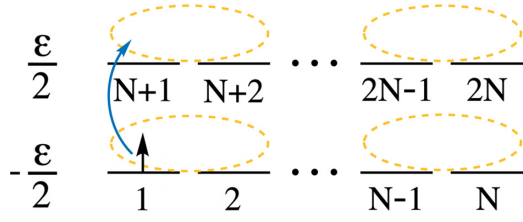


FIG. 2. A pictorial representation of the model Hamiltonian we introduce in which there are two N -degenerate energy levels—with energies $-\frac{\epsilon}{2}$ and $\frac{\epsilon}{2}$ —with double excitations and de-excitations, scattering in which one particle is de-excited while another is simultaneously excited, and a pairwise interaction term between sites $2j - 1$ and $2j$ for $j \in \{1, 2, \dots, N\}$ (yellow circles) is shown. Note that the Lipkin-like excitations must occur within a site ($p \leftrightarrow p + N$, blue arrow).

excitations and de-excitations, and the γ term allows for a single particle to be scattered up while another is simultaneously scattered down; as a result, in the Lipkin model, only even excitations are allowed, and only one particle may occupy a given site (i.e., have a specific quantum number p) such that each site in the lower level is particle-hole paired with the corresponding site in the upper level. By having the terms correlating orbitals in the Hamiltonian (λ, γ) be sufficiently larger than the energy term (i.e., in the limit of high correlation), the maximal exciton condensation— $\lambda_G = \frac{N}{2}$ [36]—can be obtained for $\lambda = \gamma$.

C. Fermion-exciton condensation

A fermion-exciton condensate is a single quantum state that simultaneously demonstrates character of superconductivity and exciton condensation, i.e., both signatures of condensation—the largest eigenvalue of the particle-particle RDM [Eq. (1)] and the largest eigenvalue of the modified particle-hole RDM [Eq. (3)]—are simultaneously large ($\lambda_D, \lambda_G > 1$) [38].

To gain insight into such fermion-exciton condensates, here we propose a model system that is capable of demonstrating simultaneous fermion-pair and exciton condensate character. In this model, we introduce the pairwise interaction from the pairing-force model into the scaffolding of the Lipkin model; thus, the model keeps the structure of the Lipkin model in which N particles occupy two N -degenerate energy levels ($-\frac{\epsilon}{2}$ and $\frac{\epsilon}{2}$) with allowed double excitations on two sites (λ) and simultaneous scattering of a particle up on one site and down on another (γ)—where Lipkin-like sites are now given as orbitals p and $p + N$; however, we additionally pair adjacent orbitals—orbitals $2j - 1$ and $2j$ for $j \in \{1, 2, \dots, N\}$ —via the PF parameter G . (See Fig. 2.) The Hamiltonian for this model is thus given by

$$\mathcal{H} = -\frac{\epsilon}{2} \sum_{i=1}^N \hat{a}_i^\dagger \hat{a}_i + \frac{\epsilon}{2} \sum_{i=1}^N \hat{a}_{i+N}^\dagger \hat{a}_{i+N} + \frac{\lambda}{2} \sum_{p=1}^N \sum_{q=1}^N \hat{a}_p^\dagger \hat{a}_q^\dagger \hat{a}_{q+N} \hat{a}_{p+N} + \frac{\lambda}{2} \sum_{p=1}^N \sum_{q=1}^N \hat{a}_{p+N}^\dagger \hat{a}_q^\dagger \hat{a}_q \hat{a}_p$$

$$+ \frac{\gamma}{2} \sum_{p=1}^N \sum_{q=1}^N \hat{a}_{p+N}^\dagger \hat{a}_q^\dagger \hat{a}_{q+N} \hat{a}_p + \frac{\gamma}{2} \sum_{p=1}^N \sum_{q=1}^N \hat{a}_p^\dagger \hat{a}_{q+N}^\dagger \hat{a}_q \hat{a}_{p+N} - G \sum_{j=1}^N \sum_{k=1}^N \hat{a}_{2j-1}^\dagger \hat{a}_{2j}^\dagger \hat{a}_{2k} \hat{a}_{2k-1} \quad (5)$$

in second quantization, with a given set of parameters ($\epsilon, \lambda, \gamma, G$) directly determining the extent of fermion-pair and exciton condensation (λ_D and λ_G , respectively) of the ground state corresponding to this model Hamiltonian.

While this model Hamiltonian is not the first to combine the pairwise interaction from the Pairing-Force model with the Lipkin model, the model Hamiltonian introduced by Plastino and coworkers causes direct competition between particle-particle and particle-hole correlations and hence proves incapable of demonstrating a fermion-exciton condensate phase (see Appendix B) [64–66]. Conversely, due to our introduction of the pairing-force interactions between adjacent orbitals instead of orbitals in the same Lipkin-like site, particle-particle and particle-hole pairing can coexist and hence fermion-pair-exciton (FEC) states can be achieved as is shown in the results that follow.

III. RESULTS

A. $N = 4$, the minimal FEC

As the authors have previously demonstrated [38], a system with as few as $N = 4$ particles in $r = 8$ orbitals can support formation of a fermion-exciton condensate. As such, we first fully explore such a minimalistic FEC system. The ground state of the FEC Hamiltonian that we have introduced—Eq. (5)—for four particles has contributions from only ten of the seventy (r choose N) possible configurations. Of these ten basis states, there are only five distinct classes composed of degenerate orientations—see Fig. 3—that allow for the direct computation of a matrix-form of the Hamiltonian in a minimal basis state. The five basis states are defined by three quantum numbers, $x, y, bool$, where the first indicates the number of particles excited to the upper energy level (x), the second indicates the number of BCS-like pairs (number of times both $2j - 1$ and $2j$ are occupied, y), and the third is a boolean that indicates whether the configuration is “Lipkin”-like in the regard that no two orbitals representing a “Lipkin” site (denoted as p and $p + N$, see the blue arrow in Fig. 3) are dually occupied or dually unoccupied.

Utilizing the basis shown in Fig. 3— $|0, 2, T\rangle$, $|2, 2, F\rangle$, $|2, 2, T\rangle$, $|2, 0, T\rangle$, and $|4, 2, T\rangle$ —the Hamiltonian from Eq. (5) can be represented by

$$\mathcal{H}_4 = \begin{pmatrix} -2\epsilon - 2G & -G\sqrt{2} & \frac{2\lambda - 2G}{\sqrt{2}} & 2\lambda & 0 \\ -G\sqrt{2} & -2G + 2\gamma & -2G & 0 & -G\sqrt{2} \\ \frac{2\lambda - 2G}{\sqrt{2}} & -2G & -2G & 2\gamma\sqrt{2} & \frac{2\lambda - 2G}{\sqrt{2}} \\ 2\lambda & 0 & 2\gamma\sqrt{2} & 2\gamma & 2\lambda \\ 0 & -G\sqrt{2} & \frac{2\lambda - 2G}{\sqrt{2}} & 2\lambda & 2\epsilon - 2G \end{pmatrix} \quad (6)$$

where each term—corresponding to the interaction between two classes of basis states, $|i\rangle$ and $|j\rangle$ —is obtained from

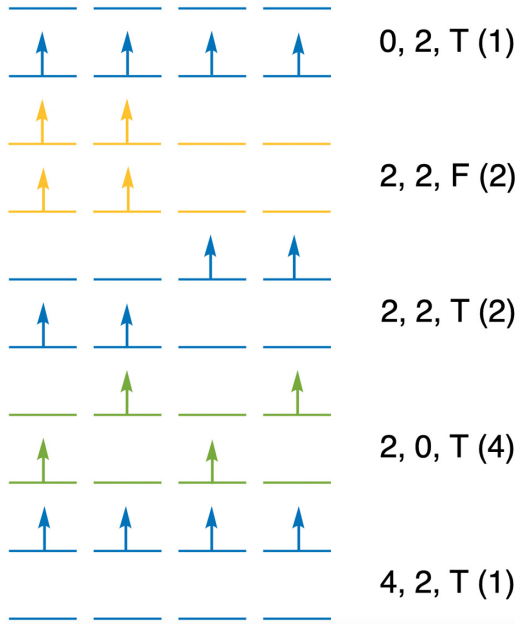


FIG. 3. Configurations representing each of the five classes of nonzero basis states for the FEC Hamiltonian for $N, r = 4, 8$ are shown where each label $x, y, bool$ represents the number of particles excited to the upper N -degenerate energy level (x), the number of BCS-like pairs (y), and whether the configuration is consistent with the Lipkin model ($bool$), where the degeneracy of each class of states is given in parenthesis, and where green, yellow, and blue configurations represent that the corresponding states are consistent with only the Lipkin Hamiltonian, only the pairing-force Hamiltonian, or both Lipkin and PF Hamiltonians, respectively.

programmatically generating all sets of second-quantization creation and annihilation operators in Eq. (5), taking the expectation value for each combination of pairs of configurations in classes $|i\rangle$ and $|j\rangle$, summing the results, and normalizing by dividing by the square root of the number of configurations for both $|i\rangle$ and $|j\rangle$. For example, if $|i\rangle = |2, 2, F\rangle = (|1, 2, 5, 6\rangle + |3, 4, 7, 8\rangle)/\sqrt{2}$ and $|j\rangle = |2, 2, T\rangle = (|1, 2, 7, 8\rangle + |3, 4, 5, 6\rangle)/\sqrt{2}$, the Hamiltonian term would be given by

$$\begin{aligned} & \frac{\langle 1, 2, 5, 6 | + \langle 3, 4, 7, 8 |}{\sqrt{2}} \mathcal{H} \frac{(|1, 2, 7, 8\rangle + |3, 4, 5, 6\rangle)}{\sqrt{2}} \\ &= \frac{1}{2} [\langle 1, 2, 5, 6 | \mathcal{H} | 1, 2, 7, 8\rangle + \langle 1, 2, 5, 6 | \mathcal{H} | 3, 4, 5, 6\rangle \\ &+ \langle 3, 4, 7, 8 | \mathcal{H} | 1, 2, 7, 8\rangle + \langle 3, 4, 7, 8 | \mathcal{H} | 3, 4, 5, 6\rangle]. \end{aligned} \quad (7)$$

Figure 4(a) scans over the signatures of condensation— λ_D and λ_G —for the ground state of the Hamiltonian in Eq. (6) by systematically varying the parameters $\epsilon, \lambda, \gamma$, and G where the yellow BCS x's represent ground states in which the PF Hamiltonian is implemented (i.e., $\lambda = \gamma = 0$), the blue Lipkin x's represent states in which the Lipkin Hamiltonian is implemented (i.e., $G = 0$), and where the green FEC x's represent states with character of both PF and Lipkin Hamiltonians. As this figure demonstrates, the largest degree of superconducting character (the largest λ_D) is indeed observed

in the BCS limit of the FEC Hamiltonian (when $G \gg \epsilon, \lambda = \gamma \approx 0$), and the largest degree of exciton condensate character (the largest λ_G) is observed in the Lipkin limit of the FEC Hamiltonian ($\lambda \approx \gamma \gg \epsilon, G \approx 0$). However, neither the BCS nor Lipkin limit of the Hamiltonian is capable of demonstrating a dual fermion-exciton condensate as λ_D and λ_G only simultaneously exceed the Pauli-like limit of one when the full FEC Hamiltonian from Eq. (5) is implemented including both BCS-like (G) and Lipkin-like (λ, γ) terms.

Our model FEC Hamiltonian, however, is capable of demonstrating a wide variety of dual condensate character as a variety of input parameters lead to ground-state configurations in which both λ_G and λ_D simultaneously exceed one. Additionally, the λ_D and λ_G values obtained by scanning over the Hamiltonian parameters [in Fig. 4(a)] demonstrate an elliptic nature consistent with the convex nature of 2-RDMs projected onto a two-dimensional space [67–69] that matches predictions for a FEC that these authors first presented in Ref. [38]. This elliptic boundary as well as the density of points in the zone corresponding to fermion-exciton condensate character indicate that the FEC model Hamiltonian introduced here is capable of spanning the entirety of the FEC region of λ_D versus λ_G space (i.e., $\lambda_D, \lambda_G > 1$).

In Ref. [38], these authors theoretically establish that in the thermodynamic limit, a possible wave function demonstrating fermion-exciton condensation can be obtained by entangling wave functions that separately demonstrate superconducting character ($|\Psi_D\rangle$ with large λ_D) and exciton condensate character ($|\Psi_G\rangle$ with large λ_G) according to

$$|\Psi_{FEC}\rangle = \frac{1}{\sqrt{2 - |\Delta|}} (|\Psi_D\rangle - \text{sgn}(\Delta)|\Psi_G\rangle), \quad (8)$$

where $\Delta = 2\langle\Psi_D|\Psi_G\rangle$. In Fig. 5, occupation probabilities for each of the five classes of basis states consistent with the $N, r = 4, 8$ FEC Hamiltonian that contribute to a BCS wave function (yellow, $\epsilon, \lambda, \gamma, G = 0, 0, 0, 0.7, \lambda_D = 1.50, \lambda_G = 0.67$), a Lipkin wave function (blue, $\epsilon, \lambda, \gamma, G = 0, -0.5, -0.5, 0, \lambda_D = 0.50, \lambda_G = 2.00$), and a FEC wave function (green, $\epsilon, \lambda, \gamma, G = 0, -0.5, -0.5, 0.7, \lambda_D = 1.31, \lambda_G = 1.32$) are given. From this data, it can be observed that the FEC wave function does indeed appear to be an entanglement of the individual BCS and Lipkin wave functions for the case of $N = 4$; this is consistent with the theoretical result in the thermodynamic limit.

B. Higher-particle FECs

In order to observe trends related to system size, we employ the methodologies used to explore the $N, r = 4, 8$ model system and extrapolate to systems composed of $N = 6, 8, 10$ particles in $r = 12, 16, 20$ orbitals. Figures summarizing the signatures of superconducting character (λ_D) and exciton condensate character (λ_G) obtained for the ground-state wave functions of these larger model Hamiltonians can be seen in Figs. 4(b)–4(d). Similar to the results from the $N = 4$ data, elliptic fits span the range from the maximal signature of superconducting character observed for the BCS wave function to the maximal signature of exciton condensate character for the Lipkin wave function, with a large variety of parameters supporting dual fermion-exciton condensation. Note that as

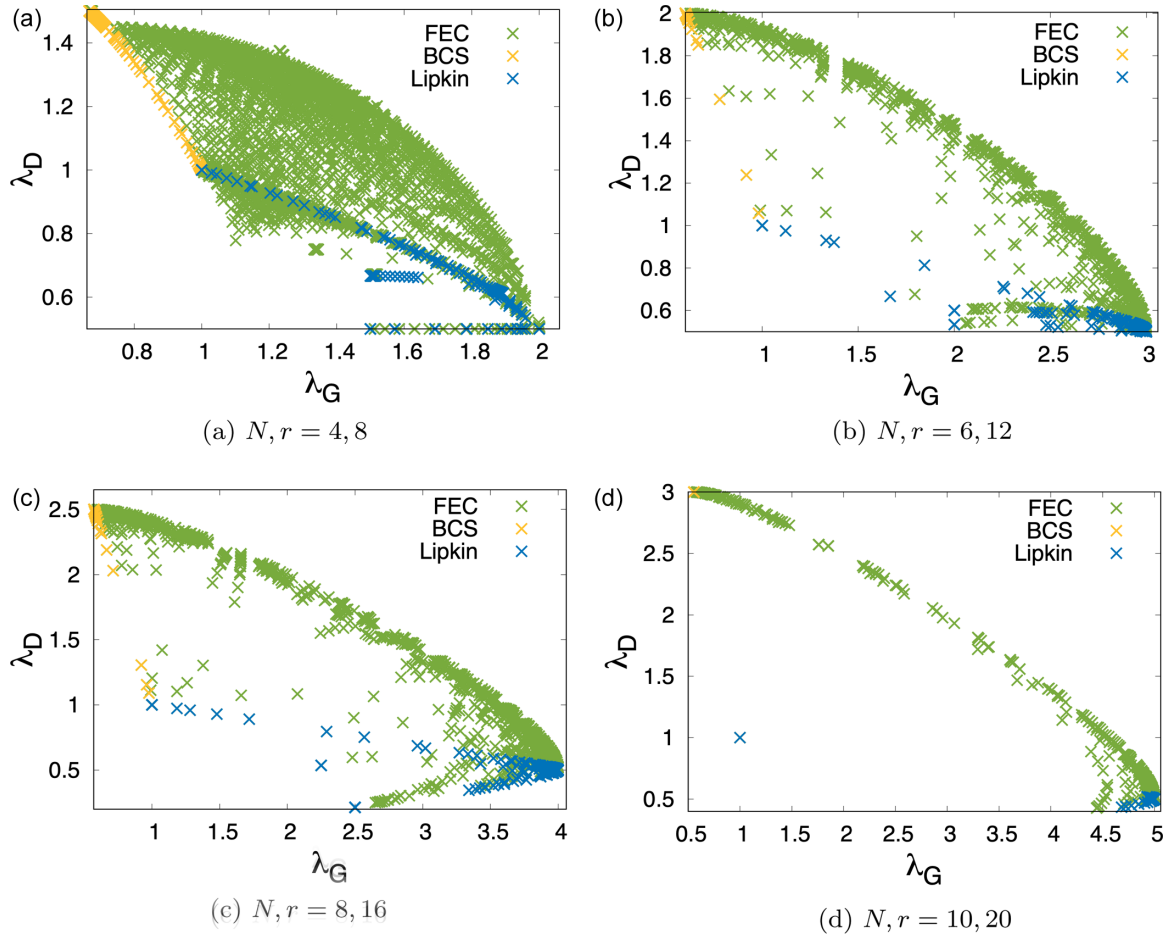


FIG. 4. Plots of λ_G vs λ_D where parameters in the FEC Hamiltonian are systematically varied are shown for systems involving (a) $N = 4$, (b) 6, (c) 8, and (d) 10 particles in $r = 2N$ orbitals.

the size of the system increases from $N = 6$ to $N = 8$ to $N = 10$, the number of classes of degenerate, nonzero basis states as well as the number of basis states composing each

class increase from 8 classes with a total of 44 nonzero basis states to 14 classes with a total of 230 nonzero basis states to 20 classes with a total of 1212 nonzero basis states. As such, the relative sparsity of the computations in λ_D versus λ_G with increasing system size is due to fewer computations being run with larger increments between each of the parameters as they are varied.

To demonstrate how the classes of nonzero basis states vary as system size is increased, Fig. 6—which shows the occupation probabilities for each of the fourteen classes of basis states consistent with the $N, r = 8, 16$ FEC Hamiltonian that contribute to a BCS wave function (yellow, $\epsilon, \lambda, \gamma, G = 0, 0, 0, 0.9$, $\lambda_D = 2.50$, $\lambda_G = 0.57$), a Lipkin wave function (blue, $\epsilon, \lambda, \gamma, G = 0, -0.5, -0.5, 0$, $\lambda_D = 0.50$, $\lambda_G = 4.00$), and a FEC wave function (green, $\epsilon, \lambda, \gamma, G = 0, -0.5, -0.5, 0.9$, $\lambda_D = 2.06$, $\lambda_G = 1.87$)—is included. Note that due to an increase in the possible complexity, two more quantum numbers are added to describe a few of the classes of basis states; specifically, ζ and τ are added to x , y , and $bool$ where ζ corresponds to the number of times BCS-like pairs are “stacked” into the same site such that orbitals $2j - 1, 2j, 2j - 1 + N$, and $2j + N$ are all occupied and where τ corresponds to the number of diagonal configurations in which either $2j - 1/2j + N$ or $2j - 1 + N/2j$ are both occupied where $2j - 1$ and $2j$ are adjacent, BCS-paired

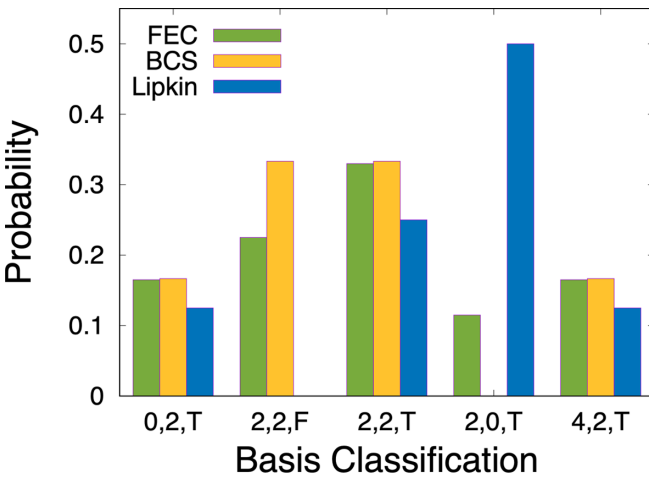


FIG. 5. The probabilities corresponding to each of the five classes of basis states (see Fig. 3) consistent with the FEC Hamiltonian for $N, r = 4, 8$ are shown where green, yellow, and blue bars correspond to the lowest eigenstate of the Lipkin Hamiltonian, the pairing-force Hamiltonian, and FEC Hamiltonian, respectively.

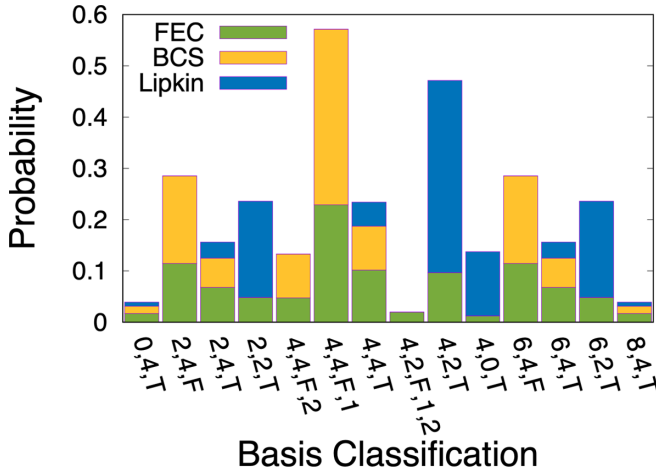


FIG. 6. The probabilities corresponding to each of the fourteen classes of basis states consistent with the FEC Hamiltonian for $N, r = 8, 16$ are shown where green, yellow, and blue bars correspond to the lowest eigenstate of the Lipkin Hamiltonian, the pairing-force Hamiltonian, and FEC Hamiltonian, respectively. Each label $x, y, bool, \zeta$, and τ represents the number of particles excited to the upper N -degenerate energy level (x), the number of BCS-like pairs (y), whether the configuration is consistent with the Lipkin model (*bool*), the number of times BCS-like pairs are “stacked” into the same site (ζ), and the number of times a diagonal configuration occur in which either $2j - 1/2j + N$ or $2j - 1 + N/2j$ are simultaneously occupied where $2j - 1$ and $2j$ are adjacent, paired orbitals (τ). These values act as quantum numbers that define the degenerate classes of nonzero basis functions composing the ground state to the FEC Hamiltonian.

orbitals. A few configurations with the necessary quantum numbers specified for $N = 8$ are included in Fig. 7.

As can be seen from Fig. 6, the ground-state wave function for the $N = 8$ FEC Hamiltonian no longer simply contains elements of the BCS wave function and the Lipkin wave function naively entangled together. Specifically, while the $|4, 4, F, 1, 2\rangle$ class of basis states does include BCS-paired particles (see Fig. 7), it does not include the maximal number

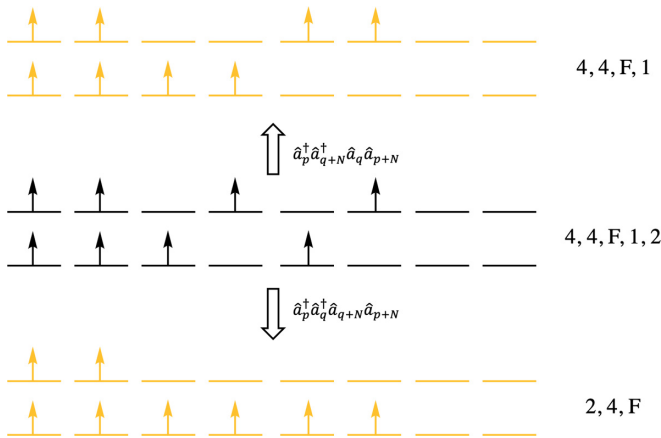


FIG. 7. Configurations representing how the Lipkin-like double excitation term (λ) and scattering term (γ) in the FEC Hamiltonian relate the $|4, 4, F, 1, 2\rangle$ basis state for $N, r = 8, 16$ to BCS-like basis states.

of BCS-paired particles, which appears to be a necessary condition for nonzero occupation of the ground state for the BCS Hamiltonian. However, this class of basis states can interact with other BCS-like and Lipkin-like classes of basis states. Explicitly, $|4, 4, F, 1, 2\rangle$ interacts with $|2, 4, F\rangle$ via $\frac{\lambda}{2} \hat{a}_p^\dagger \hat{a}_q^\dagger \hat{a}_{q+N}^\dagger \hat{a}_{p+N}$; $|4, 4, F, 1\rangle$ via $\frac{\lambda}{2} \hat{a}_p^\dagger \hat{a}_{q+N}^\dagger \hat{a}_q \hat{a}_{p+N}$; $|6, 4, F\rangle$ via $\frac{\lambda}{2} \hat{a}_{p+N}^\dagger \hat{a}_{q+N}^\dagger \hat{a}_q \hat{a}_p$; and $|2, 2, T\rangle$ via $-G \hat{a}_{2j-1}^\dagger \hat{a}_{2j}^\dagger \hat{a}_{2k} \hat{a}_{2k-1}$, which does further entangle the Lipkin-like configurations and BCS-like configurations in a nontrivial manner. As such, while the interaction between the BCS-like classes of basis states and Lipkin-like classes of basis states in the formation of the FEC ground state wave function is not as clear-cut or simple as in the $N = 4$ case, the $N = 8$ FEC wave function is still an entanglement of BCS-like and Lipkin-like terms.

A representative configuration as well as the relevant quantum numbers for all classes of basis states for the $N = 6, 8$, and 10 FEC Hamiltonians is given in Ref. [70].

IV. DISCUSSION AND CONCLUSIONS

In this study, we introduce a model Hamiltonian that successfully demonstrates the physics associated with both fermion-pair condensation and exciton condensation, as well as encompassing the phase space consisting of systems in which fermion-pair condensation and exciton condensation are simultaneously realized—a phenomenon which we term fermion-exciton condensation (FEC). Applying this model to systems composed of $N = 4, 6, 8, 10$ particles in $r = 2N$ orbitals, we confirm this fermion-exciton condensate character for a wide variety of ground-state wave functions corresponding to a diverse range of input parameters in the model Hamiltonian, additionally verifying the prediction made in a prior investigation [38] that the wave function of a fermion-exciton condensate is an entanglement of wave functions of exciton condensates and fermion-pair condensates.

The introduction of our model Hamiltonian that supports fermion-exciton condensation advances our understanding of the forces and orbital correlations necessary for the experimental construction of FEC states in real-world materials—important insights in the search for real-world materials exhibiting fermion-exciton condensate character. Depending on the interpretation of the Hamiltonian elements, this could have ramifications for fields such as traditional and molecularly scaled electronics, spin systems, and nuclear physics.

Specifically, if the orbitals in the Hamiltonian are interpreted as spin orbitals, fermion-exciton condensates simultaneously demonstrate the condensation of Cooper pairs into a single particle-particle quantum state and the condensation of electron-hole pairs into a single particle-hole quantum state; thus, superfluid Cooper pairs—resulting in superconductivity—and superfluid excitons—which are associated with the dissipationless flow of energy [32,50]—should both be present to a certain extent in FEC systems, maybe demonstrating some hybridization of the properties of superconductors and exciton condensates, which may be relevant to the fields of energy transport and electronics in both macroscopic materials and molecular-scaled systems.

Alternatively, the two Lipkin-like N -degenerate levels can be interpreted as being representative of specific spin states such that the upper level is spin up and the lower level is

spin down or vice versa. This interpretation is most-consistent with $\epsilon = 0$ —which does demonstrate FEC states for a wide variety of input parameters—, although in a magnetic field the different spin states could be separated by some nonzero energy. In this framework, the Lipkin-like terms could represent simultaneous double spin flips that are either aligned (λ) or misaligned (γ), and the pairwise pairing-force term could be seen as a favorable interaction between adjacent particles demonstrating the same spin.

Moreover, as both particle-particle (consistent with the pairing-force Hamiltonian) and particle-hole (consistent with the Lipkin Hamiltonian) are utilized in the field of nuclear physics to display the essential properties of the nuclear interaction [71–73], we can interpret our FEC Hamiltonian in this framework. In this interpretation, the particles being created and annihilated are nucleons such that the Lipkin terms are associated with the interaction of nucleons within a valence shell (γ), the mixing of particle-hole excitations with the valence configurations, and excitations of a nucleon from one valence shell to another having an energetic penalty (ϵ) [71,73]. Additionally, in this interpretation, the PF pairwise interaction is associated with the short-range portion of the nuclear interaction [71,72].

Overall, this model Hamiltonian is capable of demonstrating a wider array of collective behavior than either the Lipkin or the pairing-force models. Such a Hamiltonian will have a vast degree of applications and will be beneficial for the exploration—and for benchmarking computational

methodologies for the treatment of—the nontrivial physics of real-world material and chemical systems.

Data for this work will be made available upon reasonable request. The code used for this work is available on a public Github repository [74].

ACKNOWLEDGMENTS

D.A.M. gratefully acknowledges the U.S. National Science Foundation Grants No. CHE-1565638, No. CHE-2035876, and No. DMR-2037783 and the U.S. Department of Energy, Office of Basic Energy Sciences, under Award No. DE-SC0019215. L.M.S. also gratefully acknowledges support from NSF GRFP Grant No. DGE-1746045.

L.M.S. and D.A.M. conceived of the project, developed the theoretical framework, designed the computations, wrote the code, performed the computations, analyzed the results, and wrote the paper.

APPENDIX A: DETERMINATION OF SIGNATURES OF CONDENSATION

To determine the largest eigenvalue of the particle-particle RDM (2D), see Eq. (1)—i.e., λ_D , the signature of superconducting character—only the following $N \times N$ subblock of the full 2-RDM containing the large eigenvalue must be computed and diagonalized [49,75,76]

$$\begin{array}{c|cccc}
 & \hat{a}_0\hat{a}_1 & \hat{a}_2\hat{a}_3 & \cdots & \hat{a}_{r-2}\hat{a}_{r-1} \\
 \hline
 \hat{a}_0^\dagger\hat{a}_1^\dagger & \hat{a}_0^\dagger\hat{a}_1^\dagger\hat{a}_0\hat{a}_1 & \hat{a}_0^\dagger\hat{a}_1^\dagger\hat{a}_2\hat{a}_3 & \cdots & \hat{a}_0^\dagger\hat{a}_1^\dagger\hat{a}_{r-2}\hat{a}_{r-1} \\
 \hat{a}_2^\dagger\hat{a}_3^\dagger & \hat{a}_2^\dagger\hat{a}_3^\dagger\hat{a}_0\hat{a}_1 & \hat{a}_2^\dagger\hat{a}_3^\dagger\hat{a}_2\hat{a}_3 & \cdots & \hat{a}_2^\dagger\hat{a}_3^\dagger\hat{a}_{r-2}\hat{a}_{r-1} \\
 \vdots & \vdots & \vdots & \ddots & \vdots \\
 \hat{a}_{r-2}^\dagger\hat{a}_{r-1}^\dagger & \hat{a}_{r-2}^\dagger\hat{a}_{r-1}^\dagger\hat{a}_0\hat{a}_1 & \hat{a}_{r-2}^\dagger\hat{a}_{r-1}^\dagger\hat{a}_2\hat{a}_3 & \cdots & \hat{a}_{r-2}^\dagger\hat{a}_{r-1}^\dagger\hat{a}_{r-2}\hat{a}_{r-1}
 \end{array} \quad (A1)$$

where, again, \hat{a}_i^\dagger and \hat{a}_i are the creation and annihilation operators corresponding to the orbital with index i . Each element of this subblock of the 2-RDM is the expectation value $\langle\Psi|\hat{a}_{2j-1}^\dagger\hat{a}_{2j}^\dagger\hat{a}_{2k}\hat{a}_{2k-1}|\Psi\rangle$ obtained by programmatically applying the appropriate creation and annihilation operators to each pair of nonzero basis states composing the previously obtained ground state wave function of the Hamiltonian. As an example, for the $N, r = 4$ computations, there are ten nonzero basis elements composing five distinct classes ($|0, 2, T\rangle, |2, 2, F\rangle, |2, 2, T\rangle, |2, 0, T\rangle, |4, 2, T\rangle$) that are used to construct the Hamiltonian (see the Result section). The ground-state wave function is obtained in terms of these classes with a structure given by

$$\begin{aligned}
 |\Psi\rangle &= v_{0,2,T}|0, 2, T\rangle + v_{2,2,F}|2, 2, F\rangle + v_{2,2,T}|2, 2, T\rangle \\
 &+ v_{2,0,T}|2, 0, T\rangle + v_{4,2,T}|4, 2, T\rangle
 \end{aligned} \quad (A2)$$

where each of the classes is a weighted linear combination of the basis states composing it, i.e.,

$$|2, 0, T\rangle = \frac{|1, 3, 6, 8\rangle + |1, 4, 6, 7\rangle + |2, 3, 5, 8\rangle + |2, 4, 5, 7\rangle}{\sqrt{4}} \quad (A3)$$

Thus $\langle\Psi|\hat{a}_{2j-1}^\dagger\hat{a}_{2j}^\dagger\hat{a}_{2k}\hat{a}_{2k-1}|\Psi\rangle$ is a sum of all expectation values of the form

$$v_{c_1}v_{c_2}\langle c_1|\hat{a}_{2j-1}^\dagger\hat{a}_{2j}^\dagger\hat{a}_{2k}\hat{a}_{2k-1}|c_2\rangle, \quad (A4)$$

where c_1 and c_2 refer to each of the distinct classes of nonzero basis states and where these expectation values are sums over

$$\frac{v_{b_1}v_{b_2}}{N(c_{b_1})N(c_{b_2})}\langle b_1|\hat{a}_{2j-1}^\dagger\hat{a}_{2j}^\dagger\hat{a}_{2k}\hat{a}_{2k-1}|b_2\rangle, \quad (A5)$$

where b_1 and b_2 are the basis states composing each class, where $N(c_{b_i})$ refers to the size of the class to which basis b_i belongs, and where all possible combinations of basis states are analyzed.

Note that only $\epsilon = 0$ calculations are run for the $N, r = 10, 20$ scan such that site symmetry allows the entire matrix to be constructed from three distinct types of elements, which lowers computational expense; these element types are as follows: $\hat{a}_{2j-1}^\dagger\hat{a}_{2j}^\dagger\hat{a}_{2j}\hat{a}_{2j-1}$, $\hat{a}_{2j-1}^\dagger\hat{a}_{2j}^\dagger\hat{a}_{2k}\hat{a}_{2k-1}$, and $\hat{a}_{2j-1}^\dagger\hat{a}_{2j}^\dagger\hat{a}_{2j\pm N}\hat{a}_{2j-1\pm N}$.

The signature of superconductivity (λ_D) is then computed from the $N \times N$ subblock of the 2-RDM according to the

eigenvalue equation

$${}^2Dv_D^i = \epsilon_D^i v_D^i \quad (\text{A6})$$

with the signature corresponding the largest eigenvalue (the maximum ϵ_D^i).

The portion of the particle-hole RDM (2G) associated with a large eigenvalue is composed of submatrices of the form

| | $\hat{a}_q^\dagger \hat{a}_q$ | $\hat{a}_{q+N}^\dagger \hat{a}_q$ | $\hat{a}_q^\dagger \hat{a}_{q+N}$ | $\hat{a}_{q+N}^\dagger \hat{a}_{q+N}$ |
|---------------------------------------|---|---|---|---|
| $\hat{a}_p^\dagger \hat{a}_p$ | $\hat{a}_p^\dagger \hat{a}_p \hat{a}_q^\dagger \hat{a}_q$ | $\hat{a}_p^\dagger \hat{a}_p \hat{a}_{q+N}^\dagger \hat{a}_q$ | $\hat{a}_p^\dagger \hat{a}_p \hat{a}_q^\dagger \hat{a}_{q+N}$ | $\hat{a}_p^\dagger \hat{a}_p \hat{a}_{q+N}^\dagger \hat{a}_{q+N}$ |
| $\hat{a}_{p+N}^\dagger \hat{a}_{p+N}$ | $\hat{a}_{p+N}^\dagger \hat{a}_{p+N} \hat{a}_q^\dagger \hat{a}_q$ | $\hat{a}_{p+N}^\dagger \hat{a}_{p+N} \hat{a}_{q+N}^\dagger \hat{a}_q$ | $\hat{a}_{p+N}^\dagger \hat{a}_{p+N} \hat{a}_q^\dagger \hat{a}_{q+N}$ | $\hat{a}_{p+N}^\dagger \hat{a}_{p+N} \hat{a}_{q+N}^\dagger \hat{a}_{q+N}$ |
| $\hat{a}_{p+N}^\dagger \hat{a}_p$ | $\hat{a}_{p+N}^\dagger \hat{a}_p \hat{a}_q^\dagger \hat{a}_q$ | $\hat{a}_{p+N}^\dagger \hat{a}_p \hat{a}_{q+N}^\dagger \hat{a}_q$ | $\hat{a}_{p+N}^\dagger \hat{a}_p \hat{a}_q^\dagger \hat{a}_{q+N}$ | $\hat{a}_{p+N}^\dagger \hat{a}_p \hat{a}_{q+N}^\dagger \hat{a}_{q+N}$ |
| $\hat{a}_{p+N}^\dagger \hat{a}_{p+N}$ | $\hat{a}_{p+N}^\dagger \hat{a}_{p+N} \hat{a}_q^\dagger \hat{a}_q$ | $\hat{a}_{p+N}^\dagger \hat{a}_{p+N} \hat{a}_{q+N}^\dagger \hat{a}_q$ | $\hat{a}_{p+N}^\dagger \hat{a}_{p+N} \hat{a}_q^\dagger \hat{a}_{q+N}$ | $\hat{a}_{p+N}^\dagger \hat{a}_{p+N} \hat{a}_{q+N}^\dagger \hat{a}_{q+N}$ |

(A7)

tilted in the following manner:

| | | | |
|------------------------|------------------------|----------|------------------------------------|
| $p=0, q=0$ | $p=0, q=1$ | \dots | $p=0, q=\frac{N}{2}-1$ |
| $p=1, q=0$ | $p=1, q=1$ | \dots | $p=1, q=\frac{N}{2}-1$ |
| \vdots | \vdots | \ddots | \vdots |
| $p=\frac{N}{2}-1, q=0$ | $p=\frac{N}{2}-1, q=1$ | \dots | $p=\frac{N}{2}-1, q=\frac{N}{2}-1$ |

(A8)

In order to remove the ground-state-to-ground-state transition [to form the modified particle-hole RDM, ${}^2\tilde{G}$, see Eq. (3)],

| | $\hat{a}_q^\dagger \hat{a}_q$ | $\hat{a}_{q+N}^\dagger \hat{a}_q$ | $\hat{a}_q^\dagger \hat{a}_{q+N}$ | $\hat{a}_{p+N}^\dagger \hat{a}_{p+N}$ |
|---------------------------------------|-------------------------------|-----------------------------------|-----------------------------------|---------------------------------------|
| $\hat{a}_p^\dagger \hat{a}_p$ | ${}^1D_p[0, 0] {}^1D_q[0, 0]$ | ${}^1D_p[0, 0] {}^1D_q[0, 1]$ | ${}^1D_p[0, 0] {}^1D_q[1, 0]$ | ${}^1D_p[0, 0] {}^1D_q[1, 1]$ |
| $\hat{a}_{p+N}^\dagger \hat{a}_{p+N}$ | ${}^1D_p[0, 1] {}^1D_q[0, 0]$ | ${}^1D_p[0, 1] {}^1D_q[0, 1]$ | ${}^1D_p[0, 1] {}^1D_q[1, 0]$ | ${}^1D_p[0, 1] {}^1D_q[1, 1]$ |
| $\hat{a}_{p+N}^\dagger \hat{a}_p$ | ${}^1D_p[1, 0] {}^1D_q[0, 0]$ | ${}^1D_p[1, 0] {}^1D_q[0, 1]$ | ${}^1D_p[1, 0] {}^1D_q[1, 0]$ | ${}^1D_p[1, 0] {}^1D_q[1, 1]$ |
| $\hat{a}_{p+N}^\dagger \hat{a}_{p+N}$ | ${}^1D_p[1, 1] {}^1D_q[0, 0]$ | ${}^1D_p[1, 1] {}^1D_q[0, 1]$ | ${}^1D_p[1, 1] {}^1D_q[1, 0]$ | ${}^1D_p[1, 1] {}^1D_q[1, 1]$ |

is subtracted off from each segment defined by p and q where the one-particle density matrix (1D) is given by

| | \hat{a}_p | \hat{a}_{p+N} |
|-------------------------|-----------------------------------|---------------------------------------|
| \hat{a}_p^\dagger | $\hat{a}_p^\dagger \hat{a}_p$ | $\hat{a}_p^\dagger \hat{a}_{p+N}$ |
| \hat{a}_{p+N}^\dagger | $\hat{a}_{p+N}^\dagger \hat{a}_p$ | $\hat{a}_{p+N}^\dagger \hat{a}_{p+N}$ |

(A9)

The signature of exciton condensation (λ_G) is then obtained from the eigenvalue equation

$${}^2\tilde{G}v_G^i = \epsilon_G^i v_G^i \quad (\text{A10})$$

with the signature corresponding the largest eigenvalue (the maximum ϵ_G^i).

Again, for the $N, r = 10, 20, \epsilon = 0$ calculations, site symmetry is utilized to decrease computational expense. Only submatrices corresponding to diagonal sub-matrices $p = q$, sub-matrices for BCS-paired orbitals $p = 2j - 1, q = 2j$, and for unpaired orbitals $p = 2j - 1, q \neq p \neq 2j$ need to be computed.

APPENDIX B: PLASTINO'S MODEL

In literature that dates back to the 1960s and continues to this day, Plastino and coworkers [64–66] explore a model Hamiltonian that adds a pairing-force term to the Lipkin model in the context of nuclear physics. Introducing the Plastino pairing-force term to the Lipkin Hamiltonian from Eq. (4)—which allows for slightly more flexibility than the

formulation given in the Plastino literature as that literature is concerned only with the double excitation/de-excitation (λ) term and omits the scattering term (γ)—yields the following model Hamiltonian:

$$\begin{aligned}
\mathcal{H}_p = & -\frac{\epsilon}{2} \sum_{i=1}^N \hat{a}_i^\dagger \hat{a}_i + \frac{\epsilon}{2} \sum_{i=1}^N \hat{a}_{i+N}^\dagger \hat{a}_{i+N} \\
& + \frac{\lambda}{2} \sum_{p=1}^N \sum_{q=1}^N \hat{a}_p^\dagger \hat{a}_q^\dagger \hat{a}_{q+N} \hat{a}_{p+N} + \frac{\lambda}{2} \sum_{p=1}^N \sum_{q=1}^N \hat{a}_{p+N}^\dagger \hat{a}_{q+N}^\dagger \hat{a}_q \hat{a}_p \\
& + \frac{\gamma}{2} \sum_{p=1}^N \sum_{q=1}^N \hat{a}_{p+N}^\dagger \hat{a}_q^\dagger \hat{a}_{q+N} \hat{a}_p + \frac{\gamma}{2} \sum_{p=1}^N \sum_{q=1}^N \hat{a}_p^\dagger \hat{a}_{q+N}^\dagger \hat{a}_q \hat{a}_{p+N} \\
& - G \sum_{p=1}^N \sum_{q=1}^N \hat{a}_{p+N}^\dagger \hat{a}_p^\dagger \hat{a}_q \hat{a}_{q+N}. \quad (\text{B1})
\end{aligned}$$

While the form of this Hamiltonian is similar to the one we introduce in Eq. (5), the difference is the orbitals which the pairing-force term (G) causes to be correlated in Cooper-like pairs. Specifically, while our model Hamiltonian pairs adjacent qubits (see Fig. 2), the Plastino Hamiltonian pairs orbitals on the same Lipkin-like site in different layers (i.e., stacked orbitals p and $p + N$).

In order to determine whether the Plastino Hamiltonian is capable of probing fermion-exciton condensate character—where λ_D and λ_G simultaneously exceed the Pauli-like limit

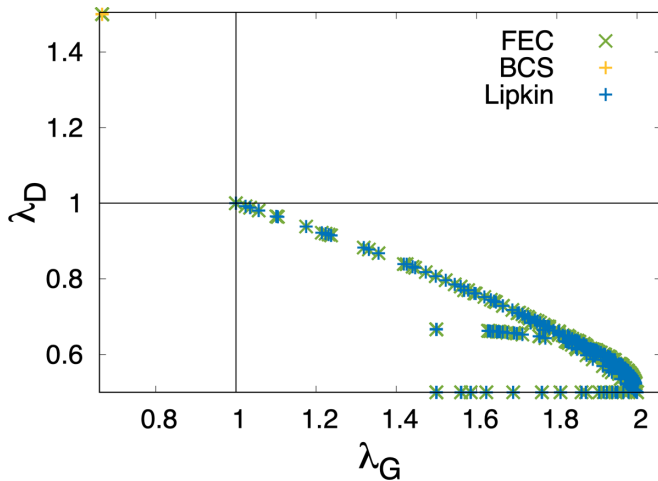


FIG. 8. A plot of λ_G vs λ_D where parameters in the Plastino Hamiltonian are systematically varied for $N = 4$ particles in $r = 8$ orbitals is shown.

of one and hence character of both fermion-pair condensation and exciton condensation are observed in a single quantum

state—a systematic scan over the input parameters of the Hamiltonian ($\epsilon, \lambda, \gamma, G$) is conducted. As can be seen by Fig. 8 where the blue pluses represent the Lipkin model Hamiltonian, the yellow pluses represent the PF BCS-like Hamiltonian, and the green x's represent the Plastino Hamiltonian, while Plastino's Hamiltonian is capable of reproducing all Lipkin states accessible by the Lipkin model and states that demonstrate fermion-pair condensation, no dual condensate character is observed from the Plastino model as the region in which both λ_D and λ_G exceed one is not probed within this model.

In fact, as noted in Ref. [66], there is direct competition between the particle-hole and particle-particle pairing between Lipkin-like sites which results in each type of pairing “driving” the system toward radically different states with the magnitudes of the coupling constants causing a transition between the Lipkin-like and BCS-like states favored by the different interactions. Conversely, because the particle-particle and particle-hole pairing in the model we introduce do not occur between the same orbitals, they can coexist, allowing for a much larger possible range of λ_D versus λ_G including the region demonstrating a fermion-exciton condensate.

- [1] K. Rabe and U. Waghmare, First-principles model Hamiltonians for ferroelectric phase transitions, *Ferroelectrics* **151**, 59 (1994).
- [2] M. Ostili and C. Presilla, The exact ground state for a class of matrix Hamiltonian models: Quantum phase transition and universality in the thermodynamic limit, *J. Stat. Mech.* (2006) P11012.
- [3] D. Debnath, M. Malik, and A. Chatterjee, A semi exact solution for a metallic phase in a Holstein-Hubbard chain at half filling with Gaussian anharmonic phonons, *Sci. Rep.* **11**, 12305 (2021).
- [4] M.-L. Cai, Z.-D. Liu, W.-D. Zhao, Y.-K. Wu, Q.-X. Mei, Y. Jiang, L. He, X. Zhang, Z.-C. Zhou, and L.-M. Duan, Observation of a quantum phase transition in the quantum Rabi model with a single trapped ion, *Nat. Commun.* **12**, 1126 (2021).
- [5] C. Farías and S. Davis, Multiple metastable states in an off-lattice Potts model, *Physica A* **581**, 126215(2021).
- [6] R. Richardson, A restricted class of exact eigenstates of the pairing-force Hamiltonian, *Phys. Lett.* **3**, 277 (1963).
- [7] R. Richardson, Application to the exact theory of the pairing model to some even isotopes of lead, *Phys. Lett.* **5**, 82 (1963).
- [8] R. Richardson and N. Sherman, Exact eigenstates of the pairing-force Hamiltonian, *Nucl. Phys.* **52**, 221 (1964).
- [9] R. W. Richardson, Exact eigenstates of the pairing-force Hamiltonian. ii, *J. Math. Phys.* **6**, 1034 (1965).
- [10] J. Bardeen, L. N. Cooper, and J. R. Schrieffer, Theory of superconductivity, *Phys. Rev.* **108**, 1175 (1957).
- [11] S. Korenblit, D. Kafri, W. Campbell, R. Islam, E. Edwards, Z.-X. Gong, G.-D. Lin, L.-M. Duan, J. Kim, K. Kim, and C. Monroe, Quantum simulation of spin models on an arbitrary lattice with trapped ions, *New J. Phys.* **14**, 095024(2012).
- [12] J. J. Hernández-Sarria, A. Argüelles, and K. Rodríguez, Quantum magnetism in spin-3/2 chains, *J. Phys.: Conf. Ser.* **614**, 012005 (2015).
- [13] D. Farnell, R. Bishop, and J. Richter, Non-coplanar model states in quantum magnetism applications of the high-order coupled cluster method, *J. Stat. Phys.* **176**, 180 (2019).
- [14] M. Środa, E. Dagotto, and J. Herbrych, Quantum magnetism of iron-based ladders: Blocks, spirals, and spin flux, *Phys. Rev. B* **104**, 045128 (2021).
- [15] H. J. Lipkin, N. Meshkov, and A. J. Glick, Validity of many-body approximation methods for a solvable model: (I.) Exact solutions and perturbation theory, *Nucl. Phys.* **62**, 188 (1965).
- [16] R. Pérez, M. C. Cambiaggio, and J. P. Vary, t expansion and the Lipkin model, *Phys. Rev. C* **37**, 2194 (1988).
- [17] N. Debergh and F. L. Stancu, On the exact solutions of the Lipkin-Meshkov-Glick model, *J. Phys. A: Math. Gen.* **34**, 3265 (2001).
- [18] D. A. Mazziotti, Exactness of wave functions from two-body exponential transformations in many-body quantum theory, *Phys. Rev. A* **69**, 012507 (2004).
- [19] W. D. Heiss, On the thermodynamic limit of the Lipkin model, *J. Phys. A: Math. Gen.* **39**, 10081 (2006).
- [20] O. Castañós, R. López-Peña, J. G. Hirsch, and E. López-Moreno, Classical and quantum phase transitions in the Lipkin-Meshkov-Glick model, *Phys. Rev. B* **74**, 104118 (2006).
- [21] G. Co' and S. De Leo, Analytical and numerical analysis of the complete Lipkin–Meshkov–Glick hamiltonian, *Int. J. Mod. Phys. E* **27**, 1850039 (2018).
- [22] J. Cioslowski, R. Erdahl, and B. Jin, On calculating approximate and exact density matrices, in *Many-Electron Densities and Reduced Density Matrices* (Kluwer Academic/Plenum, New York, 2000).
- [23] R. Xia, T. Bian, and S. Kais, Electronic structure calculations and the Ising Hamiltonian, *J. Phys. Chem. B* **122**, 3384 (2018).
- [24] A. Chu, J. Will, J. Arlt, C. Klempt, and A. Rey, Simulation of XXZ Spin Models using Sideband Transitions in Trapped Bosonic Gases, *Phys. Rev. Lett.* **125**, 240504 (2020).

- [25] A. Khamoshi, F. Evangelista, and G. Scuseria, Correlating agp on a quantum computer, *Quantum Sci. Technol.* **6**, 014004 (2021).
- [26] Z.-X. Hu, Z. Papić, S. Johri, R. Bhatt, and P. Schmitteckert, Comparison of the density-matrix renormalization group method applied to fractional quantum Hall systems in different geometries, *Phys. Lett. A* **376**, 2157 (2012).
- [27] H. Zheng, H. J. Changlani, K. T. Williams, B. Busemeyer, and L. K. Wagner, From real materials to model Hamiltonians with density matrix downfolding, *Front. Phys.* **6**, 43 (2018).
- [28] M. Al-Sugheir, M. Awawdeh, H. Ghassib, and E. Alhami, Bose-Einstein condensation in one-dimensional optical lattices: Bogoliubov's approximation and beyond, *Can. J. Phys.* **94**, 697 (2016).
- [29] L. M. Sager, S. E. Smart, and D. A. Mazziotti, Preparation of an exciton condensate of photons on a 53-qubit quantum computer, *Phys. Rev. Research* **2**, 043205 (2020).
- [30] J. von Delft, A. D. Zaikin, D. S. Golubev, and W. Tichy, Parity-Affected Superconductivity in Ultrasmall Metallic Grains, *Phys. Rev. Lett.* **77**, 3189 (1996).
- [31] M. Degroote, T. M. Henderson, J. Zhao, J. Dukelsky, and G. E. Scuseria, Polynomial similarity transformation theory: A smooth interpolation between coupled cluster doubles and projected BCS applied to the reduced BCS Hamiltonian, *Phys. Rev. B* **93**, 125124 (2016).
- [32] L. V. Keldysh, Coherent states of excitons, *Phys.-Usp.* **60**, 1180 (2017).
- [33] D. A. Mazziotti, Contracted Schrödinger equation: determining quantum energies and two-particle density matrices without wave functions, *Phys. Rev. A* **57**, 4219 (1998).
- [34] C. N. Yang, Concept of off-diagonal long-range order and the quantum phases of liquid He and of superconductors, *Rev. Mod. Phys.* **34**, 694 (1962).
- [35] F. Sasaki, Eigenvalues of fermion density matrices, *Phys. Rev.* **138**, B1338 (1965).
- [36] C. Garrod and M. Rosina, Particle-hole matrix: Its connection with the symmetries and collective features of the ground state, *J. Math. Phys.* **10**, 1855 (1969).
- [37] S. Safaei and D. A. Mazziotti, Quantum signature of exciton condensation, *Phys. Rev. B* **98**, 045122 (2018).
- [38] L. M. Sager, S. Safaei, and D. A. Mazziotti, Potential coexistence of exciton and fermion-pair condensations, *Phys. Rev. B* **101**, 081107(R) (2020).
- [39] L. M. Sager and D. A. Mazziotti, Entangled phase of simultaneous fermion and exciton condensations realized (unpublished).
- [40] S. N. Bose and A. Einstein, Planck's law and light quantum hypothesis, *Z. Phys.* **26**, 178 (1924).
- [41] A. Einstein, Quantentheorie des einatomigen idealen Gases, *Albert Einstein: Akademie-Vorträge* (John Wiley & Sons, Ltd., Hoboken, NJ, 2005), Chap. 27, pp. 237–244.
- [42] P. W. Anderson, Twenty-five years of high-temperature superconductivity – a personal review, *J. Phys.: Conf. Ser.* **449**, 012001 (2013).
- [43] A. J. Coleman, Structure of fermion density matrices, *Rev. Mod. Phys.* **35**, 668 (1963).
- [44] A. Raeber and D. A. Mazziotti, Large eigenvalue of the cumulant part of the two-electron reduced density matrix as a measure of off-diagonal long-range order, *Phys. Rev. A* **92**, 052502 (2015).
- [45] P. R. Surján, An Introduction to the Theory of Geminals, *Correlation and Localization* (Springer, Berlin, Heidelberg, 1999), pp. 63–88.
- [46] H. Shull, Natural spin orbital analysis of hydrogen molecule wave functions, *J. Chem. Phys.* **30**, 1405 (1959).
- [47] F. London, On Bose-Einstein condensation, *Phys. Rev.* **54**, 947 (1938).
- [48] L. Tisza, The theory of liquid helium, *Phys. Rev.* **72**, 838 (1947).
- [49] A. J. Coleman, Structure of fermion density matrices. ii. antisymmetrized geminal powers, *J. Math. Phys.* **6**, 1425 (1965).
- [50] D. V. Fil and S. I. Shevchenko, Electron-hole superconductivity (review), *Low Temp. Phys.* **44**, 867 (2018).
- [51] J. Kasprzak, M. Richard, S. Kundermann, A. Baas, P. Jeambrun, J. M. J. Keeling, F. M. Marchetti, M. H. Szymanska, R. André, J. L. Staehli, V. Savona, P. B. Littlewood, B. Deveaud, and L. S. Dang, Bose-Einstein condensation of exciton polaritons, *Nature (London)* **443**, 409 (2006).
- [52] M. S. Fuhrer and A. R. Hamilton, Chasing the exciton condensate, *Physics* **9**, 80 (2016).
- [53] S. Pannir-Sivajothi, J. A. Campos-Gonzalez-Angulo, L. A. Martínez-Martínez, S. Sinha, and J. Yuen-Zhou, Driving chemical reactions with polariton condensates, [arXiv:2106.12156](https://arxiv.org/abs/2106.12156).
- [54] L. V. Butov, A. Zrenner, G. Abstreiter, G. Böhm, and G. Weimann, Condensation of Indirect Excitons in Coupled AlAs/GaAs Quantum Wells, *Phys. Rev. Lett.* **73**, 304 (1994).
- [55] X. Liu, K. Watanabe, T. Taniguchi, B. I. Halperin, and P. Kim, Quantum Hall drag of exciton condensate in graphene, *Nat. Phys.* **13**, 746 (2017).
- [56] H. Min, R. Bistritzer, J.-J. Su, and A. H. MacDonald, Room-temperature superfluidity in graphene bilayers, *Phys. Rev. B* **78**, 121401(R) (2008).
- [57] Y. Cao, V. Fatemi, S. Fang, K. Watanabe, T. Taniguchi, E. Kaxiras, and P. Jarillo-Herrero, Unconventional superconductivity in magic-angle graphene superlattices, *Nature (London)* **556**, 43 (2018).
- [58] L. Sigl, F. Sigger, F. Kronowetter, J. Kiemle, J. Klein, K. Watanabe, T. Taniguchi, J. J. Finley, U. Wurstbauer, and A. W. Holleitner, Signatures of a degenerate many-body state of interlayer excitons in a van der Waals heterostack, *Phys. Rev. Research* **2**, 042044(R) (2020).
- [59] Z. Wang, D. A. Rhodes, K. Watanabe, T. Taniguchi, J. C. Hone, J. Shan, and K. F. Mak, Evidence of high-temperature exciton condensation in two-dimensional atomic double layers, *Nature (London)* **574**, 76 (2019).
- [60] M. M. Fogler, L. V. Butov, and K. S. Novoselov, High-temperature superfluidity with indirect excitons in van der Waals heterostructures, *Nat. Commun.* **5**, 4555 (2014).
- [61] A. Kogar, M. S. Rak, S. Vig, A. A. Husain, F. Flicker, Y. I. Joe, L. Venema, G. J. MacDougall, T. C. Chiang, E. Fradkin, J. van Wezel, and P. Abbamonte, Signatures of exciton condensation in a transition metal dichalcogenide, *Science* **358**, 1314 (2017).
- [62] W. Kohn and D. Sherrington, Two kinds of bosons and Bose condensates, *Rev. Mod. Phys.* **42**, 1 (1970).
- [63] A. O. Schouten, L. M. Sager, and D. A. Mazziotti, Exciton condensation in molecular-scale van der Waals stacks, *J. Phys. Chem. Lett.* **12**, 9906 (2021).

- [64] M. Cambiaggio and A. Plastino, Quasi spin pairing and the structure of the Lipkin model, *Z. Phys. A* **288**, 153 (1978).
- [65] F. Pennini and A. Plastino, Complexity and disequilibrium as telltales of superconductivity, *Physica A* **506**, 828 (2018).
- [66] A. R. Plastino, G. L. Ferri, and A. Plastino, Interaction between different kinds of quantum phase transitions, *Quantum Rep.* **3**, 253 (2021).
- [67] C. A. Schwerdtfeger and D. A. Mazziotti, Convex-set description of quantum phase transitions in the transverse Ising model using reduced-density-matrix theory, *J. Chem. Phys.* **130**, 224102 (2009).
- [68] G. Gidofalvi and D. A. Mazziotti, Computation of quantum phase transitions by reduced-density-matrix mechanics, *Phys. Rev. A* **74**, 012501 (2006).
- [69] V. Zauner, D. Draxler, L. Vanderstraeten, J. Haegeman, and F. Verstraete, Symmetry breaking and the geometry of reduced density matrices, *New J. Phys.* **18**, 113033 (2016).
- [70] See Supplemental Material at <http://link.aps.org/supplemental/10.1103/PhysRevB.105.035143> for representative configurations for all classes of basis states for the $N = 6, 8,$ and 10 FEC Hamiltonians.
- [71] P. Ring and P. Schuck, *The Nuclear Many-Body Problem* (Springer, Berlin, Germany, 2004).
- [72] M. Cambiaggio, A. Rivas, and M. Saraceno, Integrability of the pairing Hamiltonian, *Nucl. Phys. A* **624**, 157 (1997).
- [73] P. V. Isacker and K. Heyde, Exactly solvable models of nuclei, *Scholarpedia* **9**, 31279 (2014).
- [74] L. M. Sager and D. A. Mazziotti, "Simultaneous fermion and exciton condensations from a model Hamiltonian", <https://github.com/damaz/Simultaneous-Fermion-Exciton-Condensations-Model-Hamiltonian> (2022).
- [75] K. Head-Marsden and D. A. Mazziotti, Pair 2-electron reduced density matrix theory using localized orbitals, *J. Chem. Phys.* **147**, 084101 (2017).
- [76] W. Poelmans, M. Van Raemdonck, B. Verstichel, S. De Baerdemacker, A. Torre, L. Lain, G. E. Massaccesi, D. R. Alcoba, P. Bultinck, and D. Van Neck, Variational optimization of the second-order density matrix corresponding to a seniority-zero configuration interaction wave function, *J. Chem. Theory Comput.* **11**, 4064 (2015).